

ChemComm

Accepted Manuscript



This is an *Accepted Manuscript*, which has been through the Royal Society of Chemistry peer review process and has been accepted for publication.

Accepted Manuscripts are published online shortly after acceptance, before technical editing, formatting and proof reading. Using this free service, authors can make their results available to the community, in citable form, before we publish the edited article. We will replace this *Accepted Manuscript* with the edited and formatted *Advance Article* as soon as it is available.

You can find more information about *Accepted Manuscripts* in the [Information for Authors](#).

Please note that technical editing may introduce minor changes to the text and/or graphics, which may alter content. The journal's standard [Terms & Conditions](#) and the [Ethical guidelines](#) still apply. In no event shall the Royal Society of Chemistry be held responsible for any errors or omissions in this *Accepted Manuscript* or any consequences arising from the use of any information it contains.



Journal Name

COMMUNICATION

A Squaraine-based Colorimetric and F⁻ Dependent Chemosensor for Recyclable CO₂ Gas Detection: Highly Sensitive Off-On-Off Response

Received 00th January 20xx,
Accepted 00th January 20xx

DOI: 10.1039/x0xx00000x

Guomin Xia, Yang Liu, Benfei Ye, Jianqi Sun, Hongming Wang*

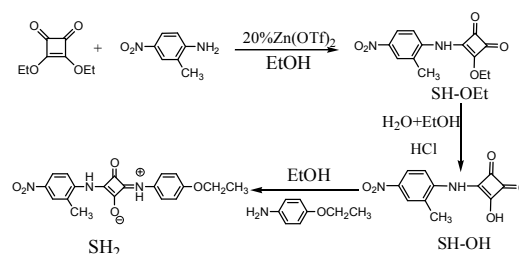
www.rsc.org/

An unsymmetrical squaraine-based chemosensor SH₂ has been synthesized, and its sensing behavior towards CO₂ gas was detailedly described by UV-vis and ¹HNMR spectroscopies in DMSO. Results indicated that the extremely sensitive “naked-eyes” CO₂ gas detection can be operated in the presence of excess [Bu₄N]⁺F⁻ (TBAF) and easy to recycle. These properties enable SH₂ to act as a CO₂ and F⁻ controlled “OFF-ON-OFF” switch. Combining theoretical analyses, a plausible sensing mechanism was proposed to illustrate how the receptor SH₂ works as a CO₂ sensitive and selective colorimetric probe in the present system.

With the constantly increasing and complicated of anthropogenic activities, the rising levels of atmospheric carbon dioxide (CO₂)¹, mostly induced by the over-consumption of carbon-based fossil fuels energy²⁻⁴, leads to and aggravates a series of natural disasters including the greenhouse effect, a rise in sea levels as well as a probable expansion of subtropical deserts⁵. As such, the exploration and development of appropriate technologies for CO₂ capture and sequestration (CCS)⁶ has become an urgent challenge over the world, especially at the mainly anthropogenic CO₂ emission sources (e.g., electricity and heat generation, transportation sector, industrial sector, etc.)⁷. Therefore, it is important to develop low-cost, sensitive, resettable sensors that can be used to quantitatively monitor the CO₂ concentration in the industrial processes and as a safeguard against their notorious effects on global climate change. Compared with traditional methods^{8,9} for gas detection, prevailed optical-based chemosensors have been widely explored in virtue of the outstanding advantage such as technical simplicity, high sensitivity and real-time detection^{10,11}. Recently, Juyoung Yoon's group has detailedly demonstrated a benzobisimidazolium-based sensor for the fluorescent and colorimetric detection of CO₂^{12a}. More recently, the same group has developed a chemical sensor for carbon dioxide based on a polydiacetylene(PDA-1), which shows that detection of CO₂ gas is accomplished either in water solution of PDA-1 or in the solid state with electrospun coatings of PDA-1

nanofibers.^{12b} In 2014, an anion-activated chemosensor system, NAP-chol 1, was reported, which permits the dissolved CO₂ to be detected in organic media via simple color changes or through ratiometric differences in fluorescence intensity.^{12c} Moreover, Tang's group has reported an AIE-based fluorescent chemosensor for quantitative detection of CO₂ gas¹³. However, the reversible optical modulation of chemosensor for the “naked-eye” detection of CO₂ gas remains a challenge.

Squaraine dyes are a class of organic dyes showing intense fluorescence, typically in the red and near-infrared region¹⁴. And they have exceptional high absorption coefficients extending from the green to the near-infrared region¹⁵. Moreover, these compounds have been extensively used as the signaling units in chemosensors and chemo dosimeters because of their absorbance, fluorescence spectra, and fluorescence quantum yields. These phenomena have been successfully applied to designing sensors for ion detection¹⁶. But there are few examples designed for CO₂ detection.¹⁷ In this work, we reported a squaraine-based chemosensor for the “naked-eye” and reversible detection of CO₂ gas in the presence of [Bu₄N]⁺F⁻.



Scheme 1. The synthesis of receptor SH₂.

In fact, researches on the side-product 1,3-orientation squaraine, compared with the well-known 1,2-substituted squaraine, were greatly hindered due to its poorer solubility and processibility. But the stronger H bond donor ability of N-H fragments makes the 1,3-isomer to be a potential candidate in the field of H bond-based anion detection. For that reason, we designed and synthesized a simple unsymmetrical 1,3-squaraine SH₂ (Scheme 1 and Synthesis of SH₂ in ESI), and the structure was confirmed by NMR, Mass, and

^aInstitute for Advanced Study and School of Chemistry, Nanchang University, 999 Xuefu Road, Nanchang, Jiangxi, 33031, China, E-mail: Hongmingwang@ncu.edu.cn.

Electronic Supplementary Information (ESI) available: Details of SH₂ preparation, characterization, computational method, FT-IR spectra, Figure S1-S11. See DOI: 10.1039/x0xx00000x

FTIR spectrometric analysis (See ESI). To our surprise, the green SH₂ solution obtained by treatment with 20 equiv of [Bu₄N]F(TBAF) in DMSO will gradually fade away into a purple in color when exposed to the air. This apparent change, fortunately, prompts us to discover a simple, highly sensitive and selective optical chemosensor for CO₂ detection, and the discrimination is even by “naked eyes” and able to be recycled easily at ambient temperature.

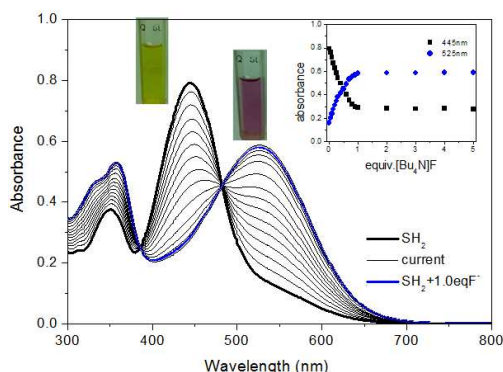


Figure 1. UV-vis spectra taken over the course of titration of receptor SH₂ (30 μM) with equivalent TBAF in DMSO. Inset: Their corresponding plots of absorbance at indicated wavelengths versus additional TBAF.

At the beginning, the affinity of receptor SH₂ toward envisaged anion (added as the tetrabutylammonium salt, TBA) was investigated by UV-vis spectroscopies. As shown in Figure 1, the absorption spectrum of the free receptor SH₂ (30 μM) displays a characteristic absorbance band centered at 445 nm in DMSO (the black line). Upon equivalent fluoride addition, the absorption band of receptor for SH₂ undergoes a significant red shift (~80 nm), and the bright-yellow solution turns into a purple in color (peak at 525 nm). These spectral changes, obviously, give rise to an isosbestic point localized at 483 nm in the absorption spectra. In the presence of 20-fold F⁻ ions, the original absorption band at 445 nm bathochromically shifted to 655 nm, and the SH₂ solution turns immediately green in colour (Figure 2). To our best knowledge, the fluoride-induced colorimetric effects, similar to the report of Taylor¹⁸, are ascribed to the enhanced acidity of the N-H fragments in the receptor SH₂. In other words, such a fluoride-detected system works in a stepwise deprotonation mechanism according to the equilibrium $\text{SH}_2 + \text{F}^- \rightleftharpoons \text{SH}^- + \text{HF}$ and $\text{SH}^- + 2\text{F}^- \rightleftharpoons \text{S}^{2-} + \text{HF}_2^-$. Further UV-Vis spectroscopic examination reveals that receptor SH₂ exhibits a highly selectivity for the F⁻ anion over other envisaged anions (see Figure S1-S4).

Unexpectedly, when the SH₂ solution obtained by treatment with 20.0 equiv of F⁻ ions was exposed to the air in an open cuvette, the intensity of the spectral feature at 655 nm was seen to decrease, while the signal at 525 nm was observed to increase in absorption spectra without stirring as time goes on (Figure 2a). The isosbestic points localized at 558 nm and the green color returns into a purple. Given a comprehensive consideration, we built a hypothesis that the atmospheric CO₂ gas responds to the discolor process in the present system. So that, increasing volumes of pure CO₂ gas (injected by tiny sampler) was bubbled into the SH₂ solution with 20-fold F⁻ ions addition in a sealed cuvette, a corresponding trend of the absorption spectra, as expected, was observed in comparison to

that exposed to the air, and the final spectrum was nearly overlapped with that of 5-fold F⁻ ions added (Figure 2b). Furthermore, it's worth noting that bubbled with only about 10 μl of CO₂ gas, the mixture was already saturated and no additional changes in the UV-Vis features were observed. The CO₂ detection limit of this system was calculated to be about 15.6 ppm (see ESI), which is lower than previous report.^{12a} Additionally, such response is quite fast and can be repeated for cycles without any change in the spectral profiles (Figure 3). These properties enable SH₂ to act as a CO₂ and F⁻ controlled “OFF–ON–OFF” switch. By alternating the addition of CO₂ gas and F⁻, the switch could be reversibly performed at least for eight cycles (Figure 3).

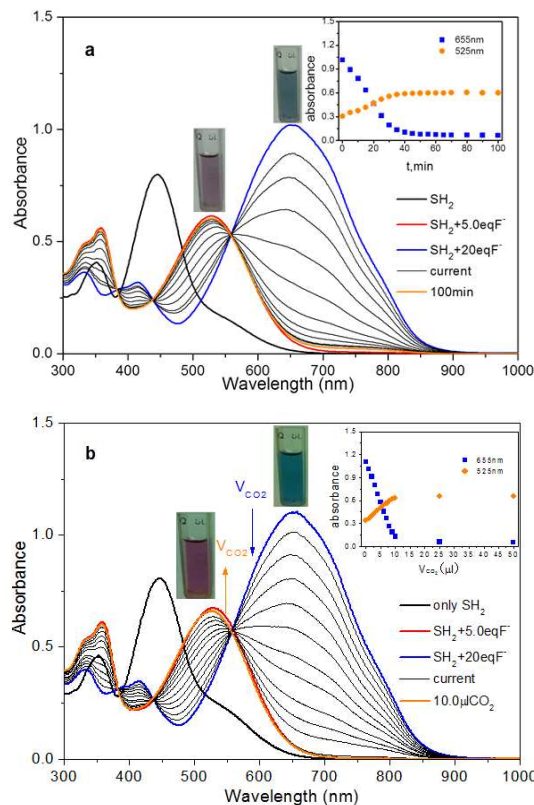


Figure 2. UV-vis spectra taken over the course of titration of receptor SH₂ (30 μM) with excess TBAF in DMSO (a) then exposed to the air in an open cuvette and (b) then bubbling with different volumes of CO₂ gas in a sealed cuvette. Inset: Their corresponding plots of absorbance at indicated wavelengths versus time or additional volume of CO₂ gas.

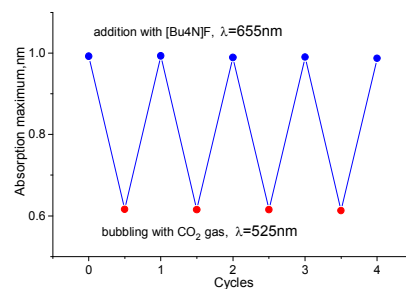


Figure 3. Reversible switching the absorption (λ_{abs}) of receptor SH₂ by repeated addition of TBAF and CO₂. More details see Figure S10.

In order to explain the electronic spectra mentioned above, theoretical calculation for the geometrical optimization of SH_2 , SH^- and S^{2-} was performed at the density functional theory (DFT) level. And also, time-dependent density functional theory (TD-DFT) calculation was performed to investigate the excited states based above optimized structures. From Figure 4, the HOMO orbitals of SH_2 , SH^- and S^{2-} are located mainly in phenetole and squarate group to form a π orbital, while the LUMO (π^*) orbitals are located mainly on nitroaniline and squarate group, respectively. For SH_2 , the peak at 445 nm in UV-vis absorption spectrum has a major contribution from HOMO (π) to LUMO (π^*) transition, which is assigned as charge transfer from phenetole to nitroaniline. In fact, the SH^- and S^{2-} have similar excited states transition. The peaks at 525 and 655nm in UV-vis absorption spectrum of SH^- and S^{2-} are also assigned as HOMO (π) to LUMO(π^*) transition, respectively. From Figure 4, the two-step deprotonation will results the level of HOMO orbital to increase largely leading to the redshift of the largest absorption peak.

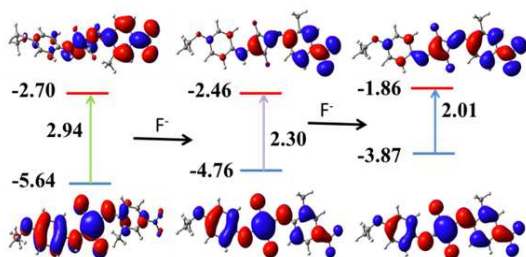


Figure 4. HOMO–LUMO energy levels of SH_2 , SH^- and S^{2-} (unit: eV).

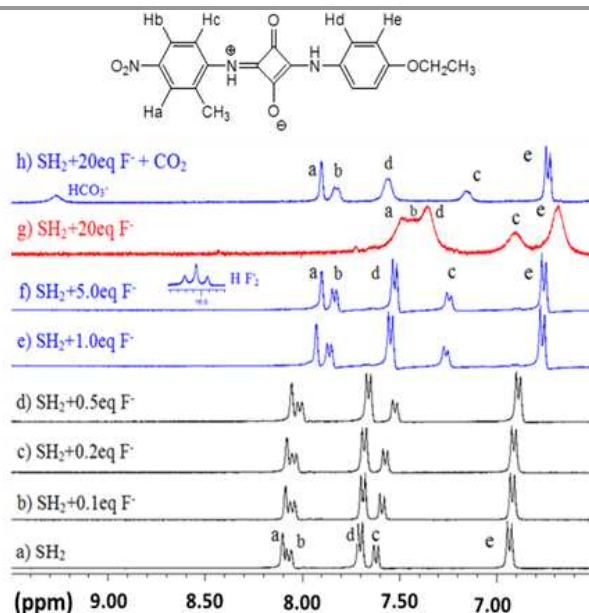
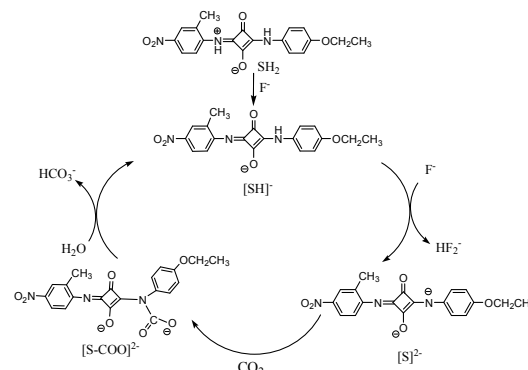


Figure 5. ^1H -NMR taken over the course of titration of receptor SH_2 (5.0mM) with TBAF followed by CO_2 in DMSO-d_6 .

Then, for a thorough insight into the underlying mechanism of the CO_2 gas recognition in the present system, ^1H NMR studies were

subsequently carried out. The family of ^1H NMR spectra taken on titration of SH_2 (5.0 mM) with TBAF followed by CO_2 gas in DMSO-d_6 is displayed in Figure 5. Upon TBAF addition (Figure 5b–5e), the signal of Hc proton underwent an upfield shift while others nearly remained unchanged, which reveals that the first N-H deprotonation is of the (2-methyl-4-nitro-) phenylamino segment. Furthermore, a new typical signal at 16.44 ppm corresponding to HF_2^- species¹⁹ could be observed in the presence of 5.0 equiv. of F^- ions (Figure 5f). All C-H protons (Ha–He) shifted upfield clearly on removal of the first proton (Figure 5e) and, in particular, the second proton (Figure 5g) in the presence of TBAF. Such distinct ^1H NMR responds are ascribed to the effect derived from the through-bond propagation onto the aromatic framework of the electronic charge generated on N-H deprotonation. Bubbling with enough CO_2 gas, the signals of all C-H protons of aromatic framework returned and a new proton signal at 9.26 ppm, which was confirmed to be HCO_3^- (Figure S6), was observed in Figure 5h. Results of ^1H NMR titrations are well consistent with those obtained from UV-vis titration experiments. Based on UV-vis and ^1H NMR spectroscopic analyses, a tentative sensing mechanism in the present system was detailedly illustrated in Scheme 2. Upon fluoride addition, the receptor SH_2 undergoes a stepwise deprotonation in DMSO according to the equilibrium $\text{SH}_2 + \text{F}^- \rightleftharpoons \text{SH}^- + \text{HF}$ and $\text{SH}^- + 2\text{F}^- \rightleftharpoons \text{S}^{2-} + \text{HF}_2^-$. However, the strong nucleophilic green S^{2-} was extremely unstable when exposed to the CO_2 gas and then it attacked CO_2 at the carbonyl to form intermediate S-COO^{2-} . Unfortunately, the putative CO_2 adduct S-COO^{2-} was not stable at ambient temperature and immediately decomposed to form the original purple SH^- and bicarbonate ions in the presence of ambient moisture²⁰. In order to give an explanation for this reaction mechanism, DFT calculation was carried out.



Scheme 2. Proposed CO_2 sensing mechanism based on the receptor SH_2 in the presence of excess TBAF.

The initial step is the first-deprotonation from SH_2 by F^- ion to form SH^- anion. The energy barrier and reaction energy for this process is $5.31 \text{ kcal mol}^{-1}$ and $-16.73 \text{ kcal mol}^{-1}$, respectively. The second-deprotonation process was carried out with energy barrier of $3.17 \text{ kcal mol}^{-1}$ and reaction energy of $-14.52 \text{ kcal mol}^{-1}$ to produce S^{2-} respectively. The low energy barrier and heat release for both deprotonation process shows that the reaction between SH_2 and F^-

is easy and fast, which is agreement with experimental observation. The following step is the addition of SH^- ion to carbon dioxide to afford the carboxylate SH-COO^- . The step holds an energy barrier of $7.65 \text{ kcal mol}^{-1}$ and endothermic heating of $2.15 \text{ kcal mol}^{-1}$, which indicates the addition of SH^- ion to carbon dioxide is hardly to carry out. However, the addition of carbon dioxide to S^{2-} ion is exothermic process by $2.65 \text{ kcal mol}^{-1}$ with an energy barrier of $1.44 \text{ kcal mol}^{-1}$ to produce S-COO^{2-} . The low energy barrier and exothermic reaction showed that the addition of carbon dioxide to S^{2-} is easy to proceed. In fact, the S-COO^{2-} is not stable in air at room temperature and able to react with water by decarboxylic reaction and gives SH^- and HCO_3^- . The energy barrier and reaction heat of this reaction are 5.79 and $-3.46 \text{ kcal mol}^{-1}$ (Figure S11). The low energy barrier shows that this reaction can carried out very easily. All above calculation can explain experimental observation that introducing CO_2 gas can result the transform of S^{2-} to SH^- but not transfer SH^- to SH_2 .

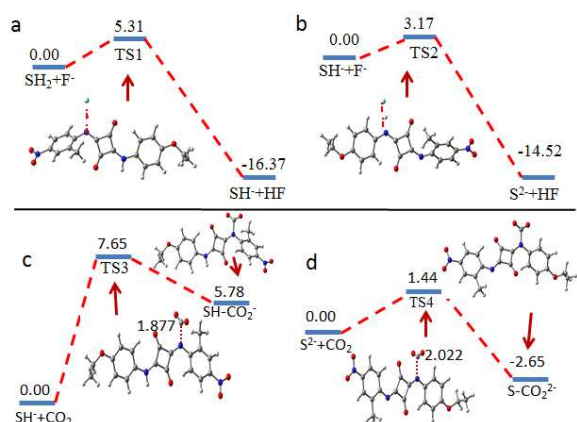


Figure 6. The reaction energy profile of CO_2 gas with SH_2 in the presence of $[\text{Bu}_4\text{N}]\text{F}$ (a: the first deprotonation step; b: the second deprotonation; c: the addition of CO_2 gas to SH^- ; d: the addition of CO_2 gas to S^{2-}) (unit for energy: kcal mol^{-1} ; unit for bond length: Å).

Conclusions

In conclusion, we have detailedly demonstrated here a squaraine-based chemosensor for the “naked-eye” detection of CO_2 gas in the presence of TBAF. The system features an operational simplicity, exceptional sensitivity, fast response times; and is able to repeat for cycles. These properties enable SH_2 to act as a CO_2 and F^- controlled “OFF-ON-OFF” switch. Furthermore, the underlying mechanism for fluoride-dependent CO_2 gas detection in the present system is particularly depicted by means of spectroscopic and theoretical analyses.

The support of the National Natural Science Foundation of China (21363014 and 21103082) is gratefully acknowledged. This work was supported by Natural Science Foundation of Jiangxi Province of China (Grant No. 20142BCB23003 and 20143ACB21021).

Notes and references

- (a) S. N. Riduan, Y. G. Zhang, *Dalton Trans.*, 2010, **39**, 3347-3357. (b) J. Tollefson, *Nature*, 2009, **462**, 966-967.
- (a) L. Yang, H. Wang, *ChemosusChem.*, 2014, **7**, 962-998. (b) L. Yang, H. Wang, N. Zhang, S. Hong, *Dalton Trans* 2013, **42**, 11186-11193. (b) G. Xia, C. Ruan, H. Wang, *Analyst*, 2015, **140**, 5099-5104.
- (a) T. Fan, X. Chen, Z. Lin, *Chem. Commun.*, 2012, **48**, 10808-10828. (b) C. S. Song, *Catal. Today*, 2006, **115**, 2-32.
- (a) W. Wang, S. Wang, X. Ma, J. Gong, *Chem. Soc. Rev.*, 2011, **40**, 3703-3727. (b) C. Finn, S. Schnittger, L. J. Yellowlees, J. B. Love, *Chem. Commun.*, 2012, **48**, 1392-1399.
- (a) W. Sattler, G. Parkin, *J. Am. Chem. Soc.*, 2012, **134**, 17462-17465. (b) C. Ziebart, C. Federsel, P. Anbarasan, R. Jackstell, W. Baumann, A. Spannenberg, M. Beller, *J. Am. Chem. Soc.*, 2012, **134**, 20701-20704. (c) C. Lescot, D. U. Nielsen, I. S. Makarov, A. T. Lindhardt, K. Daasbjerg, T. Skrydstrup, *J. Am. Chem. Soc.*, 2014, **136**, 6142-6147.
- (a) C. Song, *Catal. Today*, 2006, **115**, 2-32. (b) E. Alberico, M. Nielsen, *Chem. Commun.*, 2015, **51**, 6714-6725.
- (a) B. Koerner, J. Klopatek, *Environmental Pollution*, 2002, **116**, 45-51. (b) L. J. Murphy, K. N. Robertson, R. A. Kemp, H. M. Tuononen, J. A. C. Clyburne, *Chem. Commun.*, 2015, **51**, 3942-3956.
- S. Neethirajan, D. S. Jayas, S. Sadistap, *Food Bioprocess. Tech.*, 2009, **2**, 115-121.
- O. S. Wolfbeis, L. J. Weis, M. J. P. Leiner, W. E. Ziegler, *Anal. Chem.*, 1988, **60**, 2028-2030.
- Y. Li, Y. Wang, R. Yang, *Anal. Chem.*, 2015, **87**, 2495-2503.
- M. Vendrell, D. Zhai, Y.-T. Chang, *Chem. Rev.*, 2012, **112**, 4391-4420.
- (a) Z. Guo, N. R. Song, J. H. Moon, J. Yoon, *J. Am. Chem. Soc.*, 2012, **134**, 17846-17849. (b) Q. Xu, S. Lee, Y. Cho, M. H. Kim, J. Bouffard, J. Yoon, *J. Am. Chem. Soc.*, 2013, **135**, 17751-17754. (c) X. Zhang, S. Lee, Y. Liu, J. Yin, J. L. Sessler, J. Yoon, *Scientific Reports.*, 2014, **4**, 4593.
- Y. Liu, Y. Tang, B. Z. Tang, *J. Am. Chem. Soc.*, 2010, **132**, 13951-13953.
- (a) U. Mayerhöfer, F. Wüthner, *Chem. Sci.* 2012, **3**, 1215-1220, (b) A. Ajayaghosh, P. Chithra, R. Varghese, *Angew. Chem. Int. Ed.*, 2007, **46**, 230-233; (c) U. Mayerhöfer, F. Wüthner, *Angew. Chem. Int. Ed.*, 2012, **51**, 5615-5619; (d) S. F. Völker, C. Lambert, *Chem. Mater.*, 2012, **24**, 2541-2553. (e) S. F. Völker, A. Schmiedel, M. Holzappel, K. Renziehausen, V. Engel, C. Lambert, *J. Phys. Chem. C.*, 2014, **118**, 17467-17482.
- (a) E. Arunkumar, C. C. Forbes, B. C. Noll, B. D. Smith, *J. Am. Chem. Soc.*, 2005, **127**, 3288-3289; (b) U. Mayerhöfer, B. Fimmel, F. Wüthner, *Angew. Chem. Int. Ed.*, 2012, **51**, 164-167; (c) J. M. Baumes; J. J. Gassensmith, J. Giblin, J.-J. Lee, A. G. White, W. J. Culligan, W. M. Leevy, M. Kuno, B. D. Smith, *Nature Chem.*, 2010, **2**, 1025-1030.
- (b) Y. Xu, Z. Li, A. Malkovskiy, S. Sun, Y. Pang, *J. Phys. Chem. B.*, 2010, **114**, 8574. (b) C. Chen, R. Wang, L. Guo, N. Fu, H. Dong and Y. Yuan, *Org. Lett.*, 2011, **13**, 1162.
- E. Climent, A. Agostini, M. E. Moragues, R. Martínez-Mañez, F. Sancenón, T. Pardo, M. D. Marcos, *Chem. Eur. J.* 2013, **19**, 17301 - 17304
- A. Rostami, A. Colin, X. Y. Li, M. G. Chudzinski, A. J. Lough, M. S. Taylor, *J. Org. Chem.* 2010, **75**, 3983-3992
- Y. Xie, Q. Wang, Y. Ding, X. Li, W. Zhu, *Chem. Commun.*, 2010, **46**, 3669-3671.
- (a) E. R. Perez, R. H. A. Santos, D. W. Franco, *J. Org. Chem.*, 2004, **69**, 8005-8011. (b) C. Villiers, J.-P. Dognon, R. Pollet, P. Thury, M. Ephritikhine, *Angew. Chem. Int. Ed.*, 2010, **49**, 3465-3468.